arXiv:1007.4244v1 [cond-mat.str-el] 24 Jul 2010

Thermoelectric Power of the YbT_2Zn_{20} (T = Fe, Ru, Os, Ir, Rh, and Co) Heavy Fermions

E. D. Mun, S. Jia[a], S. L. Bud'ko, P. C. Canfield

Ames Laboratory US DOE and Department of Physics and Astronomy, Iowa State University, Ames, IA 50011, USA

(Dated: July 27, 2010)

Abstract

The thermoelectric power, $S(T)$, of the heavy fermions YbT_2Zn_{20} (T = Fe, Ru, Os, Ir, Rh, and Co) has been measured to characterize their strong electronic correlations. A large, negative, local minimum in $S(T)$ with approximately -70 μV/K is found for all compounds. From the observed local minimum, the energy scales associated with both the Kondo temperature and the crystalline electric field splitting are deduced and compared to previous specific heat measurements. At low temperatures, $S(T)$ follows a linear temperature dependence, $S(T) = \alpha T$, with an enhanced value of α which is characteristic for a heavy fermion state. In the zero temperature limit, the enhanced α value strongly correlates with the electronic specific heat coefficient, $C(T)/T$, due to the large density of states at the Fermi level.

PACS numbers: 72.15.Jf, 72.15.Qm, 75.20.Hr, 75.30.Mb

Keywords: Suggested keywords

[a] Current address : Department of Chemistry, Princeton University, Princeton, New Jersey 08544, USA

I. INTRODUCTION

In a heavy fermion (HF) Kondo lattice system, the ground state is a Fermi-liquid (FL) state constituting the Landau quasi-particles. In Ce-, Yb-, and U-based intermetallic systems the conduction electrons compensate or screen the localized moments of the f-electrons where localized electrons together with their screening cloud form quasi-particles. These quasi-particles have heavy masses, reflected in an enhanced value of the Sommerfeld coefficient, $\gamma = C(T)/T|_{T\to 0}$, at low temperatures. When f-electrons so strongly couple with conduction band there is an increased overlap of the electronic state which enhances the hybridization and band widths [1].

The FL state in HF Kondo lattice systems shows strong correlations among physical quantities. One such correlation is the Kadowaki-Woods (K-W) ratio, a relation between the electrical resistivity ($\rho(T) - \rho_0 = AT^2$) and specific heat ($C(T) = \gamma T$) [2, 3], given by the universal ratio $A/\gamma^2 = 1.0\times 10^{-5}\ \mu\Omega\mathrm{cm}/(\mathrm{mJ/mol\cdot K})^2$. Recently, systematic deviations of the K-W ratio in many HF systems (especially for Yb-based compounds) have been explained by Tsujii *et al.*, taking into account the ground state degeneracy ($N = 2j+1$) [4–6]. A FL state is also characterized by the Wilson ratio (R_W) which links γ to the Pauli susceptibility $\chi(0)$ [7–9], which is given by $R_W = \pi^2 k_B^2 \chi(0)/(j(j+1)g^2\mu_B^2\gamma^2)$, where k_B, g, and μ_B are the Boltzman constant, Lande's factor, and Bohr magneton, respectively [1]. In addition to the R_W and K-W ratio, the zero temperature limit of the thermoelectric power (TEP), $S(T)/T = \alpha$, for several correlated materials has shown a strong correlation with γ via the dimensionless ratio $q = N_A eS/\gamma T = N_A e\alpha/\gamma$ [10], where N_A is the Avogadro number and e is the carrier charge.

For Yb-based HF systems, the electrical resistivity and TEP reveal complex temperature dependencies with a local extrema. In general, these extrema are related to Kondo scattering associated with the ground state and excited states of the CEF energy levels [11–13]. The characteristic temperature of the local maximum shown in $\rho(T)$ and the local minimum developed in $S(T)$ allow for an estimate of the Kondo temperature, T_K, and the crystalline electric field (CEF) splitting, Δ/k_B, as relevant energy scales in Yb-based HF systems.

In this paper, TEP measurements on YbT_2Zn_{20} (T = Fe, Ru, Os, Ir, Rh, and Co) are presented as functions of temperature and magnetic field to evaluate the correlation between specific heat and TEP in the zero temperature limit. These compounds crystallize in the

cubic $CeCr_2Al_{20}$-type structure ($F\,d\,\overline{3}\,m$, No.227) [14] and have been reported to be HF metals with no long range order down to 20 mK [15]. In the FL regime it has been shown that the R_W and K-W ratios in this family follow the theoretical predictions with different ground state degeneracies. The TEP data of YT_2Zn_{20} (T = Fe, Co) are also presented for comparison. YFe_2Zn_{20} is one of the examples of a nearly ferromagnetic Fermi liquids (NFFL) with a highly enhanced magnetic susceptibility value at low temperatures [16], whereas YCo_2Zn_{20} shows normal metallic behavior.

II. EXPERIMENTAL

Single crystals of YbT_2Zn_{20} (T = Fe, Ru, Os, Ir, Rh, and Co) and isostructural YT_2Zn_{20} (T = Fe and Co) were grown out of excess Zn [15, 16] using standard solution growth techniques [17, 18]. The TEP was measured using a dc, alternating heating, technique that utilizes two heaters and two thermometers [19]. A Quantum Design Physical Property Measurement System provided the temperature (from 2 to 300 K) and magnetic field (up to 140 kOe) environment. For T = Fe, Rh, and Co, zero-field TEP measurements were extended down to 0.4 K, measured using the same technique [19], in a CRYO Industries of America ^{3}He system. The heat current was generated in the (111)-plane of the samples ($\Delta T \parallel (111)$) and the magnetic field was applied along the [111]-direction maintaining a transverse configuration, $\Delta T \perp \mathbf{H}$.

III. RESULTS

Figure 1 shows the TEP data for YFe_2Zn_{20} and YCo_2Zn_{20}. The temperature-dependent TEP, $S(T)$, of these compounds is similar to normal metallic systems. At 300 K, $S(T)$ of both compounds is positive and has an absolute value of $\simeq 9\,\mu$V/K for YFe_2Zn_{20} and $\simeq 5\,\mu$V/K for YCo_2Zn_{20}, and then decrease monotonically to below 25 K with decreasing temperature. With further cooling, $S(T)$ of YCo_2Zn_{20} passes through a broad peak ($\sim \Theta_D/12$ [20], where Θ_D is the Debye temperature) expected to be due to phonon-drag [21]. On the other hand, $S(T)$ of YFe_2Zn_{20} shows a local minimum around 14 K ($\sim \Theta_D/23$ [20]) that is not currently understood. The absolute value of the TEP for YFe_2Zn_{20} is much smaller than other NFFL systems. A signature of the spin fluctuation temperature, T_{sf}, has been inferred from a

shoulder in AFe$_4$Sb$_{12}$ (A = Ca, Sr, and Ba) data [22] and as a minimum developed in RCo$_2$ (R = Y, Sc, and Lu) data [23]. The minimum developed near 14 K may be related to the signature of spin fluctuation, combined with phonon-drag in the YFe_2Zn_{20} system. In the $T \rightarrow 0$ K limit, $S(T)/T$ of YFe_2Zn_{20} is larger than that of YCo_2Zn_{20} as shown in the inset of Fig. 1.

In zero field, the $S(T)$ data of the YbT_2Zn_{20} (T = Fe, Ru, Os, Ir, Rh, and Co) compounds are plotted in Fig. 2. In contrast to the isostructural Y-based compounds, $S(T)$ of the Yb-based compounds exhibits a large, negative minimum (between -70 and -40 μV/K) and the sign of $S(T)$ changing above 150 K from negative to positive (not observed in this temperature range for T = Ir). The absolute TEP values of Yb-based compounds are much larger than Y-based compounds at low temperatures, while they have a similar order of magnitude compared to Y-based compounds around 300 K. A negative, highly enhanced value of the TEP, over the temperature region measured, is typical of those found in other Yb-based Kondo lattice systems [24–26].

Figure 3 shows the low temperature $S(T)$ of YbT_2Zn_{20}. For T = Fe and Ru, a broad minimum of $\sim$ -70 μV/K is shown at the temperature $T^S_{min} \sim 22$ K. For T = Os, Ir and Rh, a similar broad minimum develops at a temperature of $T^S_{min} \sim$ 16-23 K, where the width of the peak is wider than that for T = Fe and Ru. For T = Co, $S(T)$ shows a similar temperature dependence but with the minimum shifted to $T^S_{min} \sim 4$ K and it also shows slope changes around ~ 1 K and ~ 8 K. The width of the minimum for T = Co is narrower than that for the other members of this family. Above 10 K, the absolute value of the TEP for T = Co reduces rapidly as the temperature increases and the sign of the TEP changes from negative to positive close to 150 K. For comparison, $S(T)$ curves for T = Co together with T = Fe and Rh are plotted on a semi-logarithmic scale in the inset of Fig. 2. A smaller local minimum ($\sim$ -48 μV/K) is observed for $YbOs_2Zn_{20}$. It is not clear at present if this is related to the electrical resistivity measurement that showed a larger residual resistivity in $YbOs_2Zn_{20}$ compared to other members (T = Fe, Ru, Ir, and Rh) [15]. $S(T)$ of $YbIr_2Zn_{20}$ is negative over the whole temperature range measured, the sign change from negative to positive being expected around ~ 400 K, based on a linear extrapolation of $S(T)$ above 250 K. Below 10 K (or 3 K for T = Co), $S(T)$ data for all compounds show a tendency of approaching zero and reveal linear temperature dependencies, $S(T) = \alpha T$. Since the TEP was measured down to 0.4 K for T = Fe, Rh, and Co, the linear temperature dependence of $S(T)$ is even more

clearly revealed for these compounds as shown in the inset of Fig. 3.

Figure 4 presents $S(T)/T$ of YbT_2Zn_{20} below 10 K. Since no signature of any kind of long range order down to 20 mK has been observed in the resistivity measurements [15], the zero temperature limit of $S(T)/T$ can be reliably estimated by extrapolating $S(T)$ from 2 K (or 0.4 K) to $T = 0$, where the inferred $S(T)/T|_{T\to 0}$ values for T = Fe, Ru, Os, Ir, and Rh range between -3.8 $\sim$ -10 μV/K^2. For T = Co, $S(T)/T$ value at 0.4 K reaches -42 μV/K^2 and is still decreasing (see inset of Fig. 4). By using a linear extrapolation, $S(T)/T|_{T\to 0}$ value for T = Co is found to be $\sim$-57 μV/K^2.

In Fig. 5, the results of $S(T)$ measurements at $H = 0$ and 140 kOe are shown for T = Fe, Ru and Ir. For clarity, the absolute value of the TEP is shifted by -20 μV/K for T = Ru and -40 μV/K for T = Ir. A slight change of T^S_{min} and a reduction of absolute value are seen for the $H = 140$ kOe data. Above 100 K, $S(T)$ for $H = 140$ kOe remains essentially the same as $S(T)$ for $H = 0$. In the zero temperature limit for $H = 140$ kOe data, whereas $S(T)/T$ for T = Ru remain essentially the same, $S(T)/T$ at 140 kOe for T = Fe and Ir is decreased from $\sim$-3.8 to $\sim$-6.4 μV/K^2 and from $\sim$-4 to $\sim$-6.6 μV/K^2, respectively. In the inset, the TEP measured at $T = 2.2$ K is plotted as a function of magnetic field for T = Fe, Ru, and Ir, where $\Delta S = S(H) - S(0)$. An interesting point of this result is the appearance of a maximum around $\sim$70 kOe for T = Fe and Ru and a minimum around $\sim$100 kOe for T = Ir. For T = Ir the local minimum field shown in TEP is roughly matched with the metamagnetic-like anomaly seen around $H = 120$ kOe in magnetization isotherms, $M(H)$, [27] for $\mathbf{H} \parallel [110]$. For T = Fe and Ru the $M(H)$ data at $T = 2$ K do not show any signature of metamagnetic-like behavior up to 70 kOe [28], with $M(H)$ being linear in magnetic field for both compounds. In order to clarify this point, it is necessary to measure $M(H)$ for magnetic fields higher than 70 kOe, to see whether the anomaly in $S(H)$ is related to features in magnetization or electronic data.

IV. DISCUSSION

Based on earlier thermodynamic and transport measurements of this family [15], $S(T)$ data for YbT_2Zn_{20} (T = Fe, Ru, Os, Ir, Rh, and Co) can be understood qualitatively by considering the Kondo (T_K) and CEF (Δ/k_B) effects. The compounds in this series appear to be a set of model Kondo lattice systems with varying energy scales: T_K and Δ/k_B. In Fig.

6 (a), the Kondo temperature, T_K, determined from γ [15] and local minimum temperature, T^S_{min}, observed in the zero field $S(T)$ data are plotted as a function of the transition metal, T. The value of T^S_{min} correlates strongly with the value of T_K for T = Os, Ir, Rh, and Co.

A similar trend can be found in the previously published electrical resistivity, $\rho(T)$, results [15]. For T = Co, $\rho(T)$ manifests a clear local maximum, T^ρ_{max}, around 2.4 K followed by a logarithmic temperature dependence as temperature decreases. Whereas T^ρ_{max} is clear in the $\rho(T)$ data for T = Co, $\rho(T)$ data from the other members of this family only show a clear local maximum after subtracting the resistivity data of the isostructural LuT_2Zn_{20} (T = Fe, Ru, Os, Ir, and Rh) compounds. The local maximum temperatures, T^ρ_{max}, taken from Ref. [29] are plotted in Fig. 6 (a). The variation of T^ρ_{max} follows the same trend as T^S_{min} with $T^\rho_{max} \sim 2T^S_{min}$ even for T = Fe and Ru.

In a Kondo lattice system, a single minimum developed in $S(T)$ is expected when T_K is either close to or higher than Δ/k_B. Typically, an intermediate valence system such as $YbAl_3$ [24] and $YbCu_2Si_2$ [25] and a fully degenerate Kondo lattice system such as $Yb_2Pt_6Al_{15}$ [26] exhibit a single minimum in the TEP, developing below T_K. When $T_K < \Delta/k_B$, more than one peak has been frequently observed in the TEP [25, 30–32]. The low temperature extremum is usually located close to T_K, and the high temperature extremum located at 0.4-0.6 Δ/k_B is attributed to Kondo scattering off of the thermally populated CEF levels, which is in agreement with theoretical predictions [11, 13, 33–36]. Therefore, the peak position can represent T_K and Δ/k_B as relevant energy scales in Kondo lattice systems.

For the YbT_2Zn_{20} family, T_K and the ground state degeneracy play important roles in the thermodynamic and transport properties. By considering the ground state degeneracy ($N = 8$ for T = Fe and Ru, and $N = 4$ for T = Os, Rh, Ir, and Co [15]) it is expected that $T_K \geq \Delta/k_B$ for T = Fe and Ru and $T_K \lesssim \Delta/k_B$ for T = Os, Ir, Rh, and Co. Based on this, for T = Fe and Ru, it is reasonable to assume that T^S_{min} and T^ρ_{max} simply reflect T_K; with the fully degenerate case corresponding to $N = 8$. For T = Os, Ir, Rh, and Co, the two extrema in the $S(T)$ data associated with Kondo scattering on the ground state and thermally populated CEF levels could be expected, however, only one broad peak structure is developed for T = Os, Ir, Rh, and Co. We thus expect that a single broad minimum is produced by merging more than one peak structure due to the relatively small CEF level splitting ($T_K \sim \Delta/k_B$).

To reiterate: A strong correlation between the two local extrema T^ρ_{max} and T^S_{min} develops

and remains robust even when dependence on T_K appears to break down (Fig. 6 (b)). $T^{\rho}_{max} \sim 2\,T^{S}_{min}$ for T = Fe, Ru, Os, Ir, and Rh, and for T = Os, Ir, Rh, and Co $T^{S}_{min} \sim T_K$ and $T^{\rho}_{max} \sim 2\,T_K$.

As shown in Fig. 5 the magnetic field dependence of the TEP observed in YbT_2Zn_{20} (T = Fe, Ru, and Ir) is anomalous. In the simplest case of a two band model, the carrier density of electrons, n_e, and holes, n_h, can be taken as $\frac{1}{2}n = n_e = n_h$. The diffusion TEP in magnetic field with several assumptions [37] can be expressed as

$$\Delta S = S(H) - S(0) = -S(0)\frac{\Upsilon^2 H^2 \zeta(1+\zeta)}{1+\Upsilon^2 H^2 \zeta^2}$$

where $\Upsilon = 1/nec\rho(0)$, and $\zeta = L_n/L_0$ with $L_n = \frac{1}{3}(\pi k_B/e)^2$ and $L_0 = \kappa(0)/\sigma(0)T$ (Lorentz number); $\sigma(0) = 1/\rho(0)$ and $\kappa(0)$ are the electrical conductivity and thermal conductivity, respectively, in zero magnetic field. At low temperatures $L_0 = L_n$, $\rho(0) = \rho_0$ (the residual resistivity), and the diffusion TEP in zero magnetic field is proportional to the temperature, $S(0) \propto T$. Therefore, for simple metals $\Delta S = 0$ when $T = 0$, and for very low temperatures $\Delta S \propto T$. At high temperatures $L_0 = L_n$, and $S(0)$ and $\rho(0)$ are both proportional to temperature, so that ΔS tends to zero like $1/T$ as $T \to \infty$. In general, the change in the TEP will be too small to be detected at room temperature. Since the magnetoresistance (MR) for T = Fe and Ru is positive and increases monotonically at 2 K for $\mathbf{H} \parallel [111]$ up to 140 kOe [29], the change of the TEP (ΔS) should increase or saturate with increasing magnetic field. The field dependence of the TEP is not consistent with the MR results. Generally, the phonon-drag itself is not sensitive to the applied magnetic field [21], so it is clear that neither conventional phonon-drag nor diffusion TEP of conduction electrons can account for the magnetic field dependence of the TEP in these compounds. Thus, multiple factors, such as the Kondo effect and CEF contributions, have to be considered. In order to understand the observed behavior in more detail, a theoretical analysis of the TEP as a function of field for this systems will be necessary.

Earlier thermodynamic and transport measurements [15] showed that the R_W and K-W ratios of YbT_2Zn_{20} agree well with the FL picture of the HF ground state. A clear dependence of the A/γ^2 ratio on the degeneracy N is shown in the inset of Fig. 7, where the A and γ values are taken from Ref. [15] and lines for degeneracies N are based on Ref. [6]. A Fermi liquid state can also be characterized by the ratio between γ and the zero temperature limit of $S(T)/T$ [10, 38, 39]: a "quasi universal" ratio $q = N_A eS/\gamma T$ remains

close to $q = \pm 1$ for metals and the sign of q depends on the type of carriers. Although for strongly correlated electronic materials like HF systems, a single band and single scattering process is not generally thought to be sufficient for explaining the strong correlation effects, given that $C(T)/T$ and $S(T)/T$ are most sensitive to the position of the heavy band, a quasi universal ratio is expected to hold at low temperatures [40, 41].

The experimental correlation between the zero temperature limit of $S(T)/T$ and γ for YbT_2Zn_{20} (T = Fe, Ru, Os, Ir, Rh, and Co) is presented in Fig. 7, where the phonon-drag effect is ignored since it is small. For comparison, data for several other Yb-based HF compounds are also plotted in the same figure [42]. The calculated q values of Yb-based compounds vary from -0.77 for T = Fe to -1.4 for T = Rh, which are close to the value q = -1, expected for hole-like charge carriers. As shown in the figure, each data point is close to a line represented by q = -1 which means that the zero temperature limit of $S(T)/T$ is strongly correlated to γ due to the enhanced density of state at the Fermi level; the larger density of states at the Fermi level results in a larger γ and $S(T)/T|_{T\to 0}$.

V. SUMMARY

The thermoelectric power measurements on the YbT_2Zn_{20} (T = Fe, Ru, Os, Ir, Rh, and Co) compounds are in agreement with the behavior observed in many heavy fermion Kondo lattice systems. The evolution of the local minimum in $S(T)$ and the local maximum (coherence temperature) in $\rho(T)$ with variation of the transition metals can be understood based on the energy scale of Kondo temperature in conjunction with the influence of the crystalline electric field splitting. The large value of $S(T)/T$ in the zero temperature limit can be scaled with the electronic specific heat coefficient, γ, which is reflected by a strong correlation via the universal ratio $q = N_A eS/\gamma T$ and confirms the validity of Fermi-liquid descriptions.

ACKNOWLEDGMENTS

Work at Ames Laboratory was supported by the Basic Energy Sciences, U.S. Department of Energy under Contract No. DE-AC02-07CH11358.

---

[1] A. C. Hewson, *Kondo Problem to Heavy Fermion* (Cambridge University Press, Cambridge, England, 1993).

[2] K. Kadowaki and S. B. Woods, Solid State Commun. **58**, 507 (1986).

[3] K. Miyake, T. Matsuura, and C. M. Varma, Sold State Commun. **71**, 1149 (1989).

[4] N. Tsujii, K. Yoshimura, and K. Kosuge, J. Phys.: Condens. Matter **15**, 1993 (2003).

[5] H. Kontani, J. Phys. Soc. Jpn. **73**, 515 (2004).

[6] N. Tsujii, H. Kontani, and K. Yoshimura, Phys. Rev. Lett. **94**, 057201 (2005).

[7] P. B. Weigman and A. M. Tsvelik, J. Phys. C: Solid State Phys. **16**, 2281 (1983), J. Phys. C: Solid State Phys. **16**, 2321 (1983).

[8] A. Auerbach and K. Levin, Phys. Rev. B **34**, 3524 (1986).

[9] P. A. Lee, T. M. Rice, J. W. Serene, L. J. Sham, and J. W. Wilkins, Comments Condens. Matter Phys. **12**, 99 (1986).

[10] K. Behnia, D. Jaccard, and J. Flouquet, J. Phys.: Condens. Matter **16**, 5187 (2004).

[11] A. K. Bhattacharjee and B. Coqblin, Phys. Rev. B **13**, 3441 (1976).

[12] Y. Lassailly, A. K. Bhattacharjee, and B. Coqblin, Phys. Rev. B **31**, 7424 (1985).

[13] S. Maekawa, S. Kashiba, M. Tachiki, and S. Takahashi, J. Phys. Soc. Jpn. **55**, 3194 (1986).

[14] V. M. T. Thiede, W. Jeitschko, S. Niemann, and T. Ebel, J. Alloys and Compd. **267**, 23 (1998).

[15] M. S. Torikachvili, S. Jia, E. D. Mun, S. T. Hannahs, R. C. Black, W. K. Neils, D. Martien, S. L. Bud'ko, and P. C. Canfield, Proc. Natl. Acad. Sci. U.S.A. **104**, 9960 (2007).

[16] S. Jia, S. L. Bud'ko, G. D. Samolyuk, and P. C. Canfield, Nat. Phys. **3**, 334 (2007).

[17] P. C. Canfield and Z. Fisk, Philos. Mag. B **65**, 1117 (1992).

[18] P. C. Canfield, *Solution growth of intermetallic single crystals*: *a beginner's guide* (Book Series on Complex Metallic Alloys 2010, 93-111, World Scientific Publishing Co. Pte. Ltd.).

[19] E. Mun, S. L. Bud'ko, M. S. Torikachvili, and P. C. Canfield, Meas. Sci. Technol. **21**, 055104 (2010).

[20] S. Jia, N. Ni, G. D. Samolyuk, A. Safa-Sefat, K. Dennis, Hyunjin Ko, G. J. Miller, S. L. Bud'ko, and P. C. Canfield, Phys. Rev. B **77**, 104408 (2008). Note that the Debye temperatures used in this paper are recalculated; Θ_D (YFe_2Zn_{20}) = 350 K and Θ_D (YCo_2Zn_{20}) = 344 K.

[21] F. J. Blatt, P. A. Schroeder, C. L. Foiles, and D. Greig, *Thermoelectric Power of Metals* (Plenum, New York, 1976). F. J. Blatt, A. D. Caplin, C. K. Chiang, and P. A. Schroeder. Solid State Commun. **15**, 411 (1974).

[22] T. Takabatake, E. Matsuoka, S. Narazu, K. Hayashi, S. Morimoto, T. Sasakawa, K. Umeo, and M. Sera, Physica B **383**, 93 (2006).

[23] E. Gratz and A. S. Markosyan, J. Phys.: Condens. Matter 13, R385 (2001).

[24] C. L. Foiles, J. Appl. Phys. **52**, 2217 (1981).

[25] D. Andreica, K. Alami-Yadri, D. Jaccard, A. Amato, and D. Schenck, Physica B **259-261**, 144 (1999).

[26] M. Deppe, S. Hartmann, M. E. Macovei, N. Oeschler, M. Nicklas, and C. Geibel, New J. Phys. **10**, 093017 (2008).

[27] S. Yoshiuchi, M. Toda, M. Matsushita, S. Yasui, Y. Hirose, M. Ohya, K. Katayama, F. Honda, K. Sugiyama, M. Hagiwara, K. Kindo, T. Takeuchi, E. Yamamoto, Y. Haga, R. Settai, T. Tanaka, Y. Kubo, and Y. Onuki, J. Phys. Soc. Jpn. **78**, 123711 (2009).

[28] E. Mun, unpublished data.

[29] Eundeok Mun, Ph. D. thesis, Iowa State University. In zero field, the resistivity data for YbT_2Zn_{20} compounds were taken from Ref. [15]. The resistivity data for $LuFe_2Zn_{20}$ and $LuCo_2Zn_{20}$ compounds were taken from: S. Jia, N. Ni, S. L. Bud'ko, and P. C. Canfield, Phys. Rev. B **80**, 104403 (2009). The resistivity data for LuT_2Zn_{20} (T = Ru, Os, Ir, and Rh) are unpublished.

[30] D. Huo, J. Sakurai, O. Maruyama, T. Kuwai, and Y. Isikawa, J. Magn. Magn. Mater. **226-230**, 202 (2001).

[31] H. Wilhelm and D. Jaccard, Phys. Rev. B **69**, 214408 (2004).

[32] U. Köhler, N. Oeschler, F. Steglich, S. Maquilon, and Z. Fisk, Phys. Rev. B **77**, 104412 (2008).

[33] N. E. Bickers, D. L. Cox, and J. W. Wilkins, Phys. Rev. Lett. **54**, 230 (1985).

[34] G. D. Mahan, Phys. Rev. B **56**, 11833 (1997).

[35] V. Zlatić, B. Horvatić, I. Milat, B. Coqblin, G. Czycholl, and C. Grenzebach, Phys. Rev. B **68**, 104432 (2003).

[36] V. Zlatić and R. Monnier, Phys. Rev. B **71**, 165109 (2005).

[37] E. H. Sondheimer, Proc. R. Soc. Lond. A **193**, 484 (1948).

[38] C. Grenzebach, F. B. Anders, Gerd Czycholl, and T. Pruschke, Phys. Rev. B **74**, 195119 (2006).

[39] V. Zlatić, R. Monnier, J. K. Freericks, and K. W. Becker, Phys. Rev. B **76**, 085122 (2007).

[40] K. Miyake and H. Kohno, J. Phys. Soc. Jpn. **74**, 254 (2005).

[41] H. Kontani, Phys. Rev. B **67**, 014408 (2003).

[42] The zero temperature limit of S/T and γ for YbCuAl, $YbInAu_2$, $YbAl_3$, $YbCu_2Si_2$, $YbAgCu_4$, and $YbCu_{4.5}$ are taken from the table of Ref. [10]. S/T and γ of $Yb_2Pt_6Al_{15}$ are taken from Ref. [26]. γ value of $YbNi_2B_2C$ and $YbNi_2Ge_2$ are taken from Ref. [43] and Ref. [44], respectively. The TEP data of $YbNi_2B_2C$ and $YbNi_2Ge_2$ are taken from Ref. [29].

[43] S. Li, M. C. De Andrade, E. J. Freeman, C. Sirvent, R. P. Dickey, A. Amann, N. A. Frederick, K. D. D. Rathnayaka, D. G. Naugle, S. L. Bud'ko, P. C. Canfield, W. P. Beyermann, M. B. Maple, Philos. Mag. B **86**, 3021 (2006).

[44] S. L. Bud'ko, Z. Islam, T. A. Wiener, I. R. Fisher, A. H. Lacerda, P. C. Canfield, J. Magn. Magn. Mater. **205**, 53 (1999).

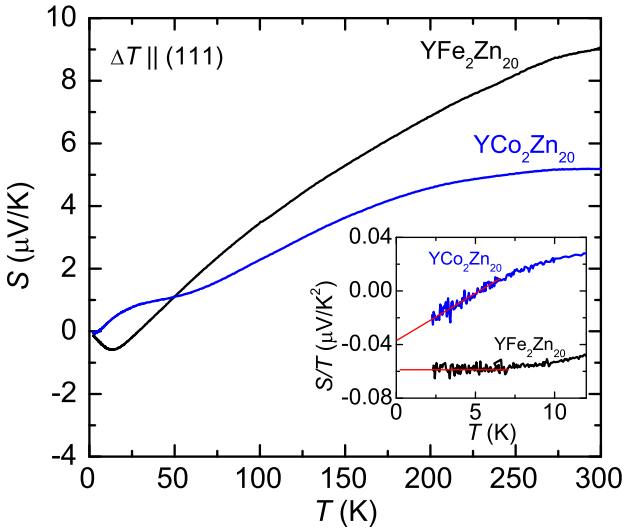

FIG. 1. Temperature-dependent thermoelectric power ($S(T)$) of YFe_2Zn_{20} and YCo_2Zn_{20} along $\Delta T \parallel (111)$. Inset: $S(T)/T$ vs. T below 12 K. Solid lines are guide to eye.

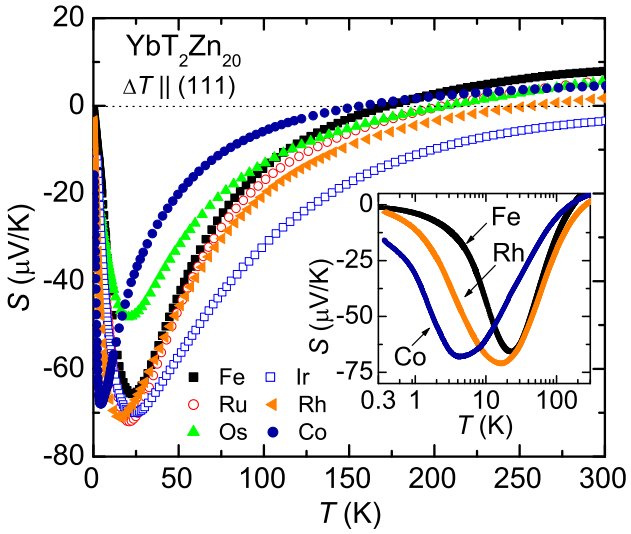

FIG. 2. Temperature-dependent thermoelectric power ($S(T)$) of YbT_2Zn_{20} (T = Fe, Ru, Os, Ir, Rh, and Co) in zero applied magnetic field. Inset: $S(T)$ vs. $\log(T)$ for T = Fe, Rh, and Co.

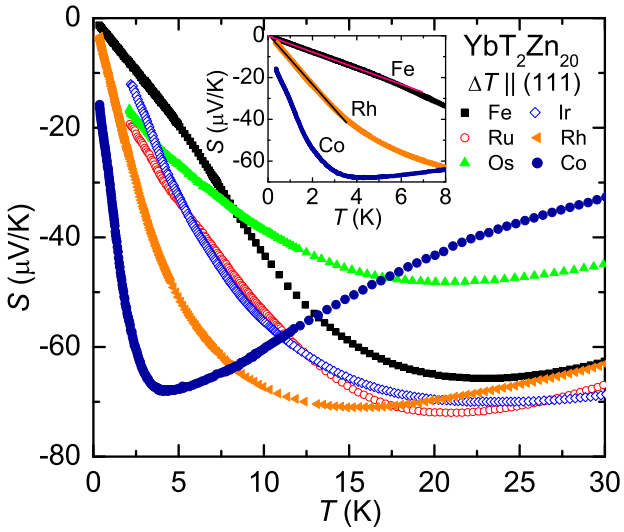

FIG. 3. Low-temperature $S(T)$ of YbT_2Zn_{20} compounds in zero applied magnetic field. Inset: $S(T)$ for T = Fe, Rh, and Co below 8 K. Solid lines on the top of the data for T = Fe and Rh are guide to eye.

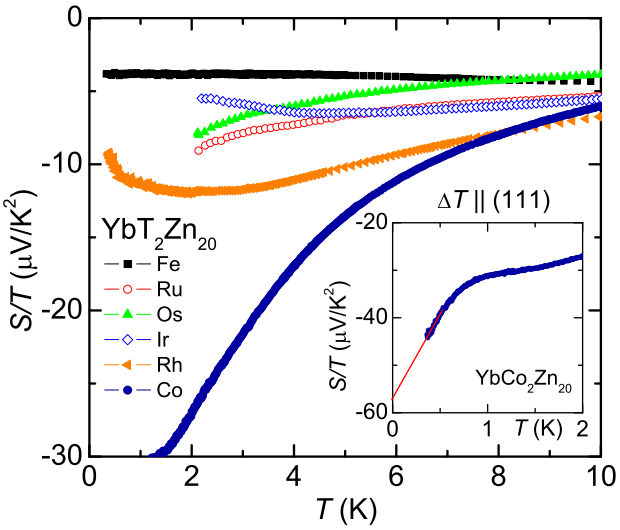

FIG. 4. $S(T)/T$ vs. T for YbT_2Zn_{20} below 10 K in zero applied magnetic field. Inset: $S(T)/T$ vs. T for $YbCo_2Zn_{20}$. The solid line represents the linear extrapolation curve to $T = 0$.

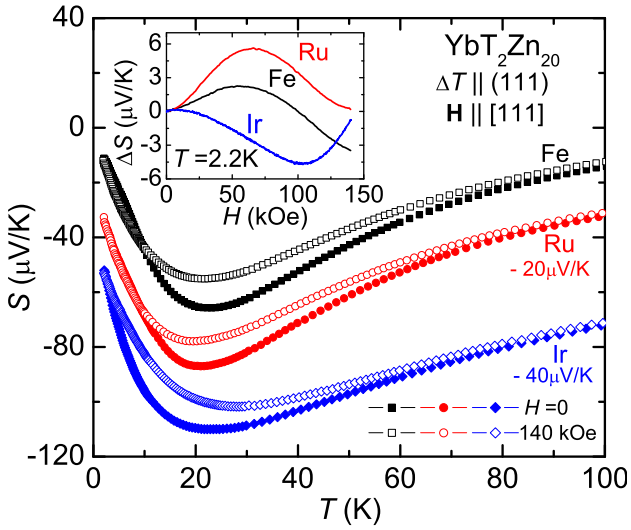

FIG. 5. $S(T)$ of YbT_2Zn_{20} (T = Fe, Ru, and Ir) at $H = 0$ (closed symbols) and 140 kOe (open symbols). For clarity, the data for T = Ru and T = Ir are shifted by -20 μV/K and -40 μV/K, respectively. Inset: $\Delta S = S(H) - S(0)$ at 2.2 K for T = Fe, Ru, and Ir.

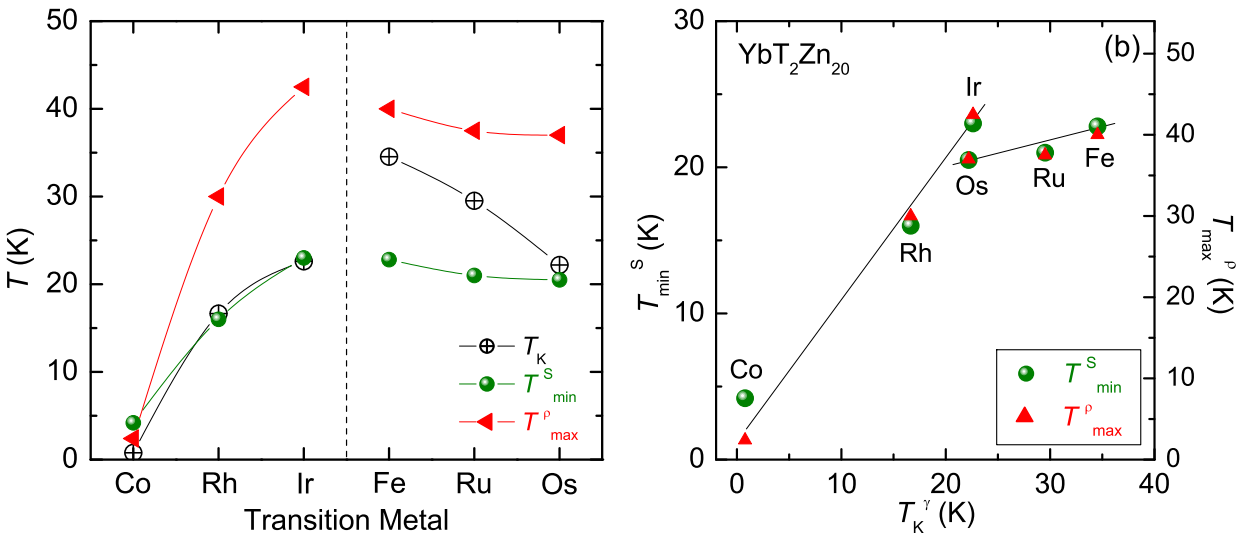

FIG. 6. (a) Relevant characteristic temperatures in YbT_2Zn_{20} (T = Fe, Ru, Os, Ir, Rh, and Co). A Kondo temperature (T_K) calculated from γ, a local maximum temperature (T^{ρ}_{max}) obtained from the resistivity, and a local minimum temperature (T^{S}_{min}) developed in $S(T)$ are plotted as a function of transition metal. T^{γ}_{K} values are taken from Ref. [15]. Vertical dashed line segregates two columns in the periodic table. (b) Plots of T^{S}_{min} (left) and T^{ρ}_{max} (right) vs. T^{γ}_{K}. Solid lines are guide to the eye.

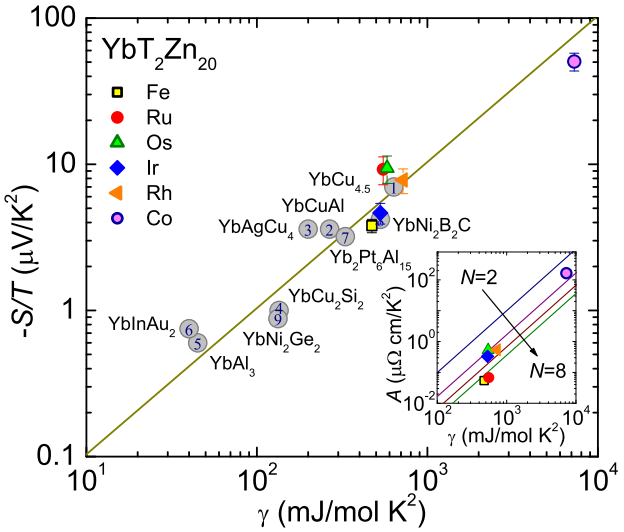

FIG. 7. -$S(T)/T|_{T\to 0}$ vs. γ (log-log) plot of YbT_2Zn_{20} (T = Fe, Ru, Os, Ir, Rh, and Co). The zero temperature limit of $S(T)/T$ and γ for (1) $YbCu_{4.5}$, (2) YbCuAl, (3) $YbAgCu_4$, (4) $YbCu_2Si_2$, (5) $YbAl_3$, and (6) $YbInAu_2$ are taken from the table of Ref. [10]. $S(T)/T$ and γ of (7) $Yb_2Pt_6Al_{15}$ are taken from Ref. [26]. $S(T)/T$ and γ of (8) $YbNi_2B_2C$ and (9) $YbNi_2Ge_2$ are taken from Refs. [42–44], respectively. The solid line represents $\gamma/(eN_A)$. Inset: Kadowaki-Woods plot (log-log plot of A vs. γ) of YbT_2Zn_{20}. Symbols are taken from Ref. [15] and solid lines correspond to $N = 2$, 4, 6, and 8 based on Ref. [6], respectively.